Amphiphilic reactive poly(glycidyl methacrylate)-block-poly(dimethyl siloxane)-block-poly(glycidyl methacrylate) triblock copolymer for the controlling nanodomain morphology of epoxy thermosets

Quan Zhou*, Qi Liu, Ning Song, Jingyi Yang, Lizhong Ni

Key Laboratory of Specially Functional Polymeric Materials and Related Technology of Ministry of Education, School of Materials Science and Engineering, East China University of Science and Technology, Shanghai 200237, China

ABSTRACT

The amphiphilic reactive tricopolymer Poly(glycidylmethacrylate) -b-Poly(dimethylsiloxane)-b-Poly(glycidylmethacrylate) (PGMA-b-PDMS-b-PGMA) was synthesized via atom transfer radical polymerization (ATRP) from the PDMS macro-initiator and glycidylmethacrylate (GMA). The internal structure of the reactive tricopolymer was described by Fourier transform infrared spectroscopy (FITR), nuclear magnetic resonance spectroscopy (NMR) and gel permeation chromatography (GPC). The PGMA-b-PDMS-b-PGMA consisted of reactive epoxy-miscible PGMA blocks, which can been involved in the cross-linking network by covalent bonds, and an epoxy-immiscible PDMS block, which separated to give the nanostructures. The morphology of the nanostructure thermosetting blends before and after curing was not much different and as well as the difference in miscibility between its subchains, inferring the formation followed the self-assembly mechanism. Static contact angle measurement and differential scanning calorimetry (DSC) indicated that the hydrophobic and the glass transition temperature were significantly increased by introducing the reactive triblock copolymer.

1. Introduction

As a matrix of various materials and fiber-reinforced as well as adhesive, epoxy resin has a widely range of uses and profound research significance [1–5].{Sánchez-Hidalgo, 2018 #10;He, 2012 #11;Qiu, 2017 #12} However, it is brittle after curing due to its large internal stress so that the ability of block copolymers to form nanodomain in epoxy thermosetting has extensive research heat in recent years [6–9]. It is well-documented that following the self-assembly [10–15] or reaction-induced microphase separation (RIMPS) [16–20], nano-morphological structures can be formed according to different solubility of segments with the resin matrix. According to the first route above, the copolymers possessing the characteristics of amphiphilic and reactive compounds is self-assembled to form various vesicle structures [21–25]. That is, the nano-sized micelle structure is selected by the substrate to form a template, and is fixed via the crosslinking of reactive components. Bates et al. [26,27] report a strategy for thermoset nanostructures provided by amphiphilic block copolymers. Zheng et al. [28–29] proposed the behavior of ordered or disordered nanostructures in thermoset resins prepared by reaction-induced microphase separation, contrary to self-assembly, all of the subchains of the block copolymers are miscible with the epoxy precursors, thus no nanodomain appears before the curing reaction. At elevated temperatures, a part of the subchains are separated out, while other blocks maintain compatibility with the thermosets.

The formation of nanostructures by introducing linear and star block copolymer into thermoset has attracted a lot of scholars' attention [30–33]. Zheng et al. [34] reported a diblock polymer poly(ε-caprolactone)-block-poly(n-butyl acrylate) (PCL-b-PBA) synthesized by ring-opening polymerization (ROP) and atom transfer radical polymerization (ATRP), in which, the nanodomain morphology transferred from spherical particles to lamellar objects with increasing the content of PBA. Zhou et al. [35,36] investigated the nanostructures in epoxy thermosets containing ABA triblock copolymer, e.g., poly(ε-caprolactone)-block-poly(ether sulfone)-block-poly(ε-caprolactone) (PCL-b-PES-b-PCL). Nanostructures in the thermosets via reaction-induced microphase separation during the elevated temperatures while phase and morphology transitions occurred with increasing amount of triblock copolymer, and the average distance between neighboring domains decreased with spherical particle of the PCL microdomains mutually integrated. Builes et al. studied [37] the relationship between the morphology of nanostructured modified with poly(ethylene oxide)-b-

poly(propylene oxide)-b-poly(ethylene oxide) (PEO-b-PPO-b-PEO) triblock copolymer and their optical and mechanical properties.

For this purpose, PEO and PCL have been the most common miscible-matrix blocks, which maintain intermolecular hydrogen bonding with epoxy thermosets. However, this strategy shifts the Tg values of the ternary thermosetting nanomaterial to a low temperature, due to the interpenetrated nonreactive blocks acting as plasticiser. In order to overcome this problem, introduction reactive sites to the epoxy-miscible block was a remarkable method [38–40]. Rebizant et al. [38] studied using polystyrene-b-polybutadiene-b-poly(methyl methacrylate)-b-poly(glycidyl methacrylate) copolymers (SBMG) to modify epoxy resins. And the properties and morphologies of epoxy resin with an epoxy-reactive poly(n-butyl acrylate)–co-poly(methyl methacrylate)–co-(glycidyl methacrylate) (BMG) diblock copolymers were studied by He et al.[39], revealing that the toughening effect and increasing of the impact strength were due to the chemical structures of relatively symmetrical copolymers. Garate et al. [40] recently studied morphological evolution of nanostructured epoxy thermosets containing with controlling epoxidation of poly(styrene-b-isoprene-b-styrene) block copolymer.

In this work, we synthesized a novel ABA triblock copolymer, amphiphilic reactive poly(glycidylmethacrylate)-b-poly(dimethylsiloxane)-b-poly (glycidyl methacrylate) (PGMA-b-PDMS-b-PGMA); the obtained thermosetting nanodomain was fixed by a curing agent DDS. The ABA triblock copolymers are designed based on the following knowledge that (a) PDMS has been extensively used as attractive synthetic precursors for versatile materials because of the high temperature resistance and flexibility of silicon-oxygen bonds. Meanwhile, PDMS can't dissolve in epoxy. (b) Oppositely, PGMA is inter-miscible with epoxy, what's more, the GMA chain cross-linking with curing agent enables the coherence of covalent linkage between copolymer and three cross-linked network, this is, the mechanical and thermal properties of thermosetting nanodomain blends containing the triblock copolymer should be improved. Therefore, the modification of epoxy with triblock copolymer containing PDMS (elastomeric block) and PGMA (reactive block) appears to be a promising approach for obtaining high performance thermosetting materials with attractive mechanical and heat resistant characteristics [41,42].

Therefore, the purpose of this work is twofold: to synthesize a new triblock copolymer by ATRP derived from PDMS, containing epoxy groups capable of reacting with curing agent DDS at a elevated temperature, and to study its application as modifier to obtain nanostructured epoxy thermosets with controlled nanodomain morphology. Such studies would contribute to a better insight into the molecular mechanism responsible for the nanodomain formation and evolution in nanostructured thermosetting materials.

2. Experimental section

2.1. Materials

The epoxy precursor diglycidyl ether of bisphenol A (DGEBA, E-51) with epoxide equivalent of 172–176 and curing agent 4,4′-diaminodiphenyl sulfone (DDS) were purchased from Aldrich Chemical Co., China. Dihydroxy-terminated polydimethylsiloxane (OH-PDMS-OH) with viscosity of 500 mPa s and monomer glycidyl methacrylate (GMA) as well as triethylamine (TEA) were obtained from Shanghai Aladdin Bio-Chem Technology Co., LTD. Prior to use, the tetrahydrofuran (THF) was further distilled under reduced pressure, which supplied by Sinopharm Chemical Reagent Co., LTD. The catalyst, cuprous chloride (CuCl) was washed by glacial acetic acid for 24 h and dried in vacuum at least 48 h. In this work, all other reagents such as N,N,N′,N′,N″-pentamethyldiethylenetr-iamine (PMDETA), 2-bromoisobutyryl bromide were obtained from Shanghai Linfeng Chemical Reagent Co., China.

2.2. Synthesis of Br-PDMS-Br macro-initiator

The difunctional macro-initiator Br-PDMS-Br was prepared with 2-bromoisobutyryl bromide in the presence of TEA [42]. Typically, PDMS (10.0 g, 2.34 mmol) and TEA (0.47 g, 4.67 mmol) were dissolved in 150 mL dry THF in a 250 mL three-neck round-bottom flask equipped with a condenser, a gas inlet/outlet, a rubber septum, and a magnetic stirrer. This system was connected to the Schlenk line system to eliminate traces of oxygen and moisture by freeze-pumpthaw cycles. The 2-bromoisobutyryl bromide (1.07 g, 4.67 mmol) was introduced into the flask after the system was cooled to 0 °C. After half an hour, the temperature was rose to 24 °C and the reaction lasted 24 h. The solution was filtered by rotary evaporation to obtain a crude product. The crude product was first dissolved in THF, and then purified in methanol (−19 °C) after washing with distilled water to obtain a pale yellow liquid (9.50 g) with the yield of 92.07%.

2.3. Synthesis of PGMA-b-PDMS-b-PGMA triblock copolymer

PGMA-b-PDMS-b-PGMA triblock copolymer was synthesized via ATRP in the present of complex formed by CuCl with PMDETA as catalyst and Br-PDMS-Br as the initiator. Typically, macro-initiator Br-PDMS-Br (10.0 g, 2.18 mmol), CuCl (0.43 g, 4.37 mmol), PMDETA (0.76 g, 4.37 mmol), GMA (8.53 g, 60.0 mmol) and 80 mL toluene were transferred into a 250 mL four-necked flask with mechanical stirrer. The system was connected to a Schlenk system and passed through three cryogenic pumps to eliminate traces of oxygen and moisture, then the reactive system was lasted at 50 °C for 3 h. The crude product was diluted with 320 mL toluene, and then the catalyst was isolated from the system by passing a neutral alumina column. The obtained liquid was precipitated in petroleum ether and dissolved in dichloromethane (CH_2Cl_2), eventually purified in excess petroleum ether to obtain the precipitate. The PGMA-b-PDMS-b-PGMA triblock copolymer was dried at 40 °C under vacuum for 48 h and a yellow solid (15.44 g) was obtained with the yield of 82.06%.

2.4. Preparation of nanostructured epoxy thermosets

The PGMA-b-PDMS-b-PGMA triblock copolymer was added to DGEBA, which was stirred evenly at 135 °C until the triblock was dissolved, and continue to stir with adding a stoichiometric amount curing agent DDS until the system was transparent again. The ternary mixture was subsequently poured into preheated Teflon molds and cured at 130 °C for 2 h plus 160 °C for 4 h plus 200 °C for 2 h.

3. Measurement and characterization

### 3.1. Fourier transform infrared spectroscopy (FT-IR)

All the samples attached to KBr disk were measured at room temperature with a Nicolet 5700 spectrometer. Liquid sample was spin-coating on the KBr disk, and solid samples were mixed with KBr powder to grind evenly to prepare KBr disks. The measured spectra ranged from 450 to 4000 cm^{-1} with a resolution of 0.09 cm^{-1}.

3.2. Nuclear magnetic resonance spectroscopy (NMR)

The samples been dissolved in tetrachloromethane (CCl_4), was measured by the AVANCE 500 Superconducting Fourier Transform NMR spectrometer with tetramethylsilane (TMS) as the internal reference, in which the frequency was 500 MHz for ^{1}H NMR and 125.77 MHz for ^{13}C NMR.

3.3. Gel permeation chromatography (GPC)

The molecular weights and molecular weight distribution (M_w/M_n)
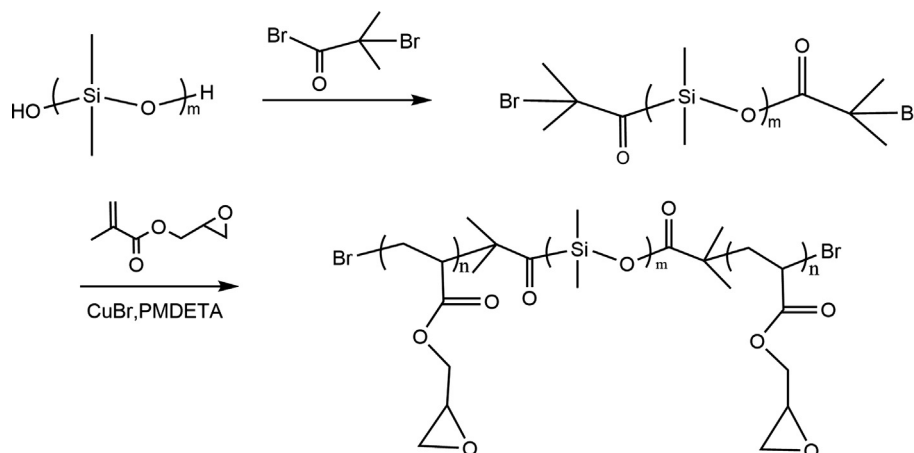
Scheme 1. Synthesis of PGMA-b-PDMS-b-PGMA triblock copolymer.

of polymers were measured by a Waters Model 1515 Chromatograph with THF as the solvent at the elution rate of 1.0 mL min^{-1} and polystyrene (PS) as a standard.

3.4. Differential scanning calorimetry (DSC)

The samples (about 5–10 mg of cured DGEBA/PGMA-PDMS-PGMA) were taken in a crucible for testing under nitrogen at a temperature ranging from 25 °C to 300 °C with a heating rate of 10 K min^{-1} by a NETZSCH DSC 200 F3 differential scanning calorimetry. The midpoint of the heat capacity change was the glass transition temperature (Tg) of the system.

3.5. Dynamic mechanical thermal anaylsis (DMTA)

The dynamic mechanical tests of 60 × 12 × 3 mm^3 samples were performed on a TA instruments DMA Q800 dynamic mechanical thermal analyzer with 3.0 H$_Z$ frequency at a heating rate of 5 °C min^{-1} range from −100 to 250 °C.

3.6. Thermal gravimetric analysis (TGA)

The thermal stability was performed on a NETZSCN TG209F1 thermal gravimetric analyzer taken on about 5–10 mg samples from 25 to 800 °C on the heating rate of 10 K min^{-1} in the nitrogen atmosphere.

3.7. Atomic force microscopy (AFM)

The surface topography information of sample was presented by the DI/MultiMode. The test used a 125 mm probe to collect images at 500 kHz frequency with tapping mode.

3.8. Scanning electron microscope (SEM)

The featured surface of sample was presented by Hitachi S-3400N field emission scanning electron microscope at an activation voltage of 15 kV. The cured modified DGEBA/PGMA-PDMS-PGMA thermosetting resin samples were made into small pieces, which were stuck on the sample stage with conductive adhesive. The gold was sprayed into the instrument for testing.

3.9. Small-angle X-ray scattering (SAXS)

Material microstructure was taken by a small-angle X-ray scattering beamline of an Anton Paar small-angle X-ray Scattering system with two-dimensional scattering image of the CCD tester image enhancement. The experiments were carried out at 40 kV voltage and 40 mA

electric current with Cu Kα radiation (λ = 0.15418 nm) at 25 °C. The scattering intensity curve can be obtained by plotting the scattering vector (q) with the scattering intensity (I),q = (4π/λ)sin(θ/2) (θ = scattering angle).

3.10. Fracture toughness test (K_{IC})

Mechanical fracture behavior of the mixture systems were performed in a three-point bending geometry with a crosshead speed of 2 mm min^{-1}. The DDS-cured DGEBA/PGMA-PDMS-PGMA blends were made into 60 × 12 × 6 mm^3 splines and the span was 48 mm. V-shaped notches with 0.25 w depth was made in each sample with a rotary cutter and a starter crack was triggered by the razor blade (the total length of the crack and the notch ranged from 0.55 to 0.65 w) according to ASTM D-5045-95. The value of K_{IC} was calculated using the following formula:

$$K_{IC} = f \frac{LP}{bw^{3/2}} \tag{1}$$

where L is the span length, b is the thickness of the sample and w is the width of the sample, which derived from measuring splines. What's more, f is the size factor and p is the maximum breaking load at crack initiation.

3.11. Tensile properties

Tensile strength was determined according to GB/T 2567-2008 on a 2KW CMT 2203 universal tensile machine at a loading rate of 5 mm min^{-1}.

4. Results and discussion

4.1. Synthesis of PGMA-b-PDMS-b-PGMA triblock copolymer

The route of synthesis for PGMA-b-PDMS-b-PGMA triblock copolymer was summarized in Scheme 1. The dihydroxyl-terminated PDMS was employed to react with 2-bromoisobutyryl bromide to afford the macroinitiator Br-PDMS-Br for the polymerization of GMA via ATRP to obtain PGMA-b-PDMS-b-PGMA triblock copolymer. ATRP was a beauty strategy for the formation of ABA triblock copolymer using a transition metal complex catalyst (CuCl/PMDETA) [43,44]. During the initiation process, cuprous ions took bromine from the macroinitiator to obtain free radicals PDMS and high-priced copper ions. In the chain growth process, a dynamic reversible balance was established between a low concentration of growing radicals PDMS and a high concentration of high-priced copper ions in order to keep the uniform growth of the PGMA chains and PGMA-b-PDMS-b-PGMA triblock copolymer was
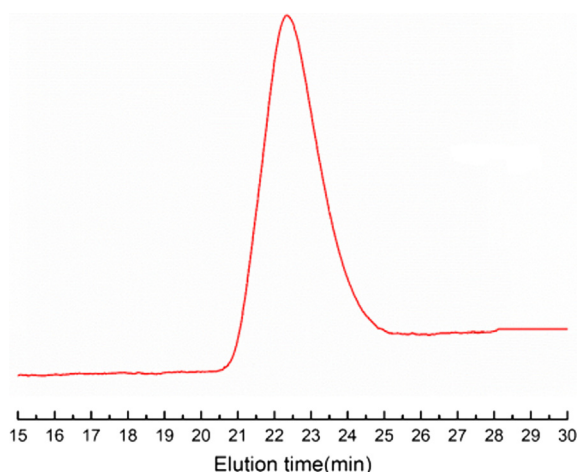
Fig. 1. The GPC curve of PGMA-b-PDMS-b-PGMA triblock copolymer.

obtained eventually [45–49]. The molecular weight of the product was $M_n = 13265$ g/mol ($M_w/M_n = 1.12$) measured by GPC (Fig. 1).

The FITR spectra of this triblock copolymer, macroinitiator Br-PDMS-Br and raw material PDMS is shown in Fig. 2. The disappearance of the hydroxyl bond at 3300 cm^{-1} indicates that the hydroxyl group in PDMS had reacted with 2-bromoisobutyryl bromide and the macroinitiator Br-PDMS-Br has been successfully synthesized. The two absorption bands of 802 cm^{-1} and 1093 cm^{-1} corresponded to stretching vibration of C-Si-C and Si-O-Si, respectively. The intensification of the stretching vibration band of carbonyl groups at 1734 cm^{-1} comparing with Br-PDMS-Br macroinitiator is ascribed to GMA monomer. Also, the asymmetrical stretching vibration of epoxy group is present at 906 cm^{-1} and the phenomenon that the C=C absorption peak at 1620 cm^{-1} is not appeared, indicating the successful introduction of PGMA block (Fig. 2c).

Fig. 3 shows the chemical structure of the triblock copolymer monitored by ^1H NMR spectrum, such as 1.8 and 2.7 ppm belonging to 3 protons of CH$_3$ and 2 protons of CH$_2$ moieties in GMA repeat units, respectively. The sharp peak at 3.6 and 4.1 ppm correspond to 2 protons of COOCH$_2$ and 3.4 ppm corresponds to the epoxy group hydrogen protons, which are belonging to PGMA block. The resonance signals center at 0.2 ppm is attributed to methyl hydrogen protons of PDMS block. Shown in Fig. 4, the ^{13}C NMR spectrum of the triblock copolymer, the protons of CH$_2$ and CH$_3$ of PDMS block are identified in 65.32, 63.04 and 52.11 ppm. A sharp signal at 173.09 ppm is assigned to carbonyl and the signal at 7.12, 26.07, 77.12 ppm are assigned to
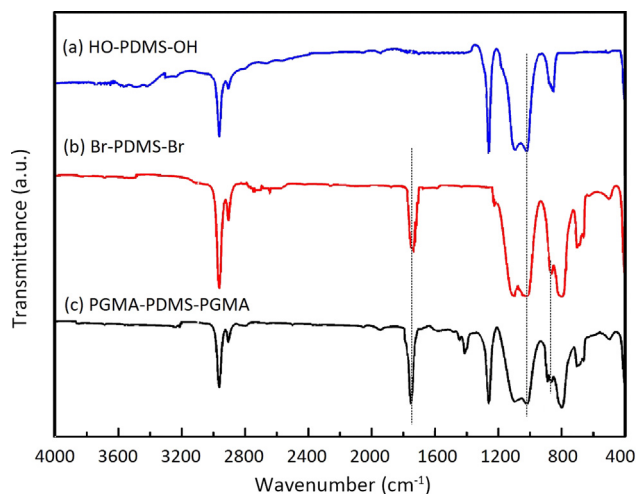

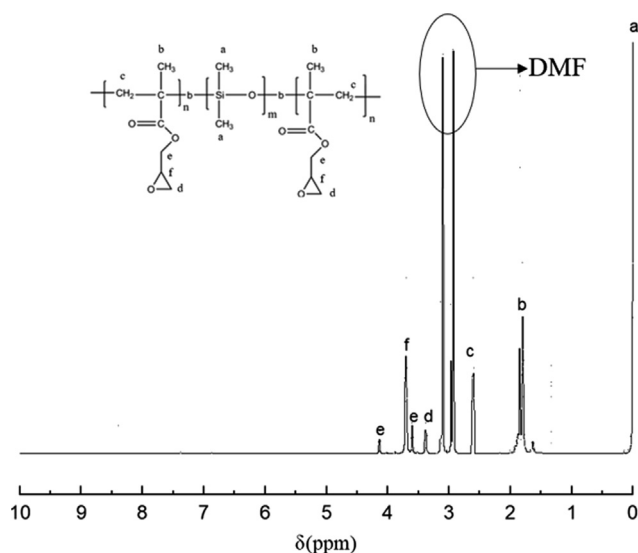**Fig. 2.** The FTIR spectrum of PDMS, Br-PDMS-Br, PGMA-b-PDMS-b-PGMA.

Fig. 3. The ^1H NMR spectrum of PGMA-b-PDMS-b-PGMA triblock copolymer.
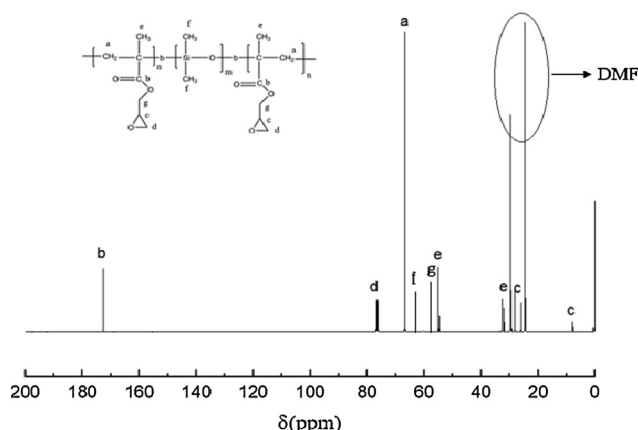

Fig. 4. The ^{13}C NMR spectrum of PGMA-b-PDMS-b-PGMA triblock copolymer.

epoxy group of GMA macromonomer. The proton resonance characteristic of PDMS and PGMA segment occurred simultaneously in NMR, indicating the successful link of the triblock component in the polymer. The length of PGMA block (L$_{PGMA}$) can be calculated from the integrated intensity ratio of the methylene protons in −Si(CH$_3$)$_2$O− and those in epoxy peak, and the L$_{PGMA}$ was 7168 g mol^{-1}, which was closed to the design structure. The results of the FTIR, NMR spectroscopy and GPC indicated that the control over the structure of the PGMA-b-PDMS-b-PGMA triblock copolymer was successfully obtained.

4.2. Nanostructures of epoxy thermosets containing PGMA-b-PDMS-b-PGMA

DGEBA/PDMS blends were cloudy at room temperature before curing reaction and the thermosets kept the turbid state after curing at elevated temperature, while the system DGEBA/PGMA was always homogeneous and transparent before and after curing. All the thermosets containing the triblock copolymer up to 25 wt% showed a transparent state, indicating that no macroscopic phase separation occurred at least on the scale exceeding the wavelength of visible light.

The microscopic surface topography of the cured DGEBA/PGMA-PDMS-PGMA system was observed by SEM as showed in Fig. 5. The composition of the darker section was attributed to the epoxy resin whereas the brighter section was the PGMA-b-PDMS-b-PGMA domain. In the DDS-cured DGEBA thermoset, the surface of the system was a
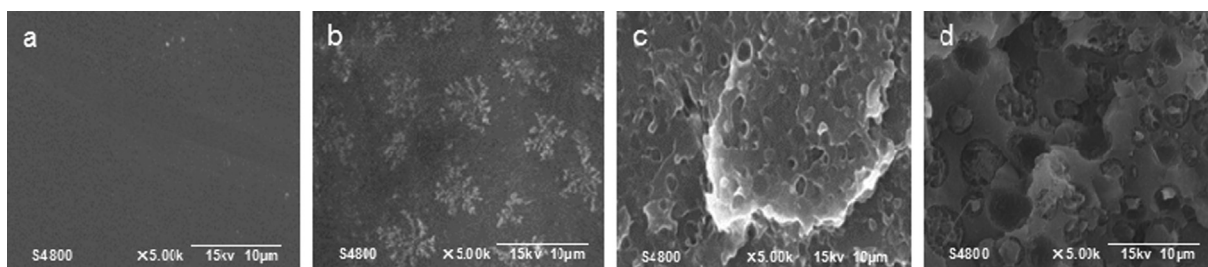
Fig. 5. The SEM images of the epoxy thermosets containing (a) 0, (b) 5, (c) 15, (d) 25 wt% of PGMA-b-PDMS-b-PGMA triblock copolymer.

single homogeneous state (Fig. 5a). The structure of the epoxy thermoset containing 5 wt% PGMA-b-PDMS-b-PGMA was presented in Fig. 5b in which it was obvious that the snowflake microphase separation structure has appeared. When the amount of triblock copolymer addition was small, the PGMA block was sufficiently extend without contact between each other to form a snowflake nanostructure. With thermosets containing 15 wt% PGMA-b-PDMS-b-PGMA triblock copolymer, the nanophases showed a distinct hole structure with a diameter of about 50–60 nm suggesting the presence of a nanophase structure in DGEBA/PGMA-PDMS-PGMA blends (Fig. 5c). As for 25 wt% DGEBA/PGMA-PDMS-PGMA blends, the nanophases were organized into a spherical structure with a smooth edge and the average diameter of the holes is 80 nm (Fig. 5d). It was seen that the mechanism of microphase separated morphologies formation was spontaneous and self-assembly due to the large difference in solubility parameters between the subchains and the epoxy resin, which was further investigated by means of AFM.

Shown in Fig. 6 are the AFM spectra of the DGEBA thermosets containing PGMA-b-PDMS-b-PGMA triblock copolymer. Based on the content of triblock copolymer in the matrix and the difference in intermolecular force of DGEBA, PGMA and PDMS, it can be judged that the dark continuous phase can be attributed to the cross-linked thermoset network whereas the bright regions correspond to the PDMS-rich micro-domains. It can be judged that the dark continuous phase can be attributed to the cross-linked epoxy network and compatible PGMA sub-chains whereas the bright regions correspond to the PDMS-rich domains. Fig. 6b showed the morphology of 5 wt% DGEBA/PGMA-PDMS-PGMA blends. It was obvious that PDMS block formed a spherical and phase-separated structure with size 50–80 nm, implying the snowflake nanostructure was evenly distributed in the continuous thermosetting resin matrix. With the concentration of triblock copolymer increasing to 15 wt%, it was noted that the nanophase has transformed from spherical into vesicle structure. As can be seen from Fig. 6d, the adjacent micro-domains of 20 wt% DGEBA/PGMA-PDMS-PGMA blends tended to be interconnected, which was consistent with the SEM results in the size of surface nanodomain.

The nanodomains structure of DGEBA/PGMA-PDMS-PGMA blends were further investigated by SAXS and the result was presented in Fig. 7. Well-defined scattering peaks can be observed in the cured system, which indicated that the thermosets possessed nanoscaled
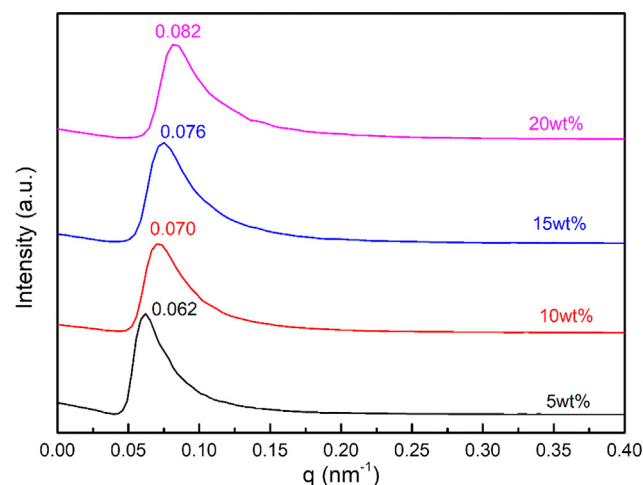

Fig. 7. SAXS curves of the epoxy thermosets containing PGMA-b-PDMS-b-PGMA triblock copolymer.

structures. According to the position of the primary scattering maximum and the Bragg scattering equation ($L = 2\pi/q_m$), the average distance between neighboring microdomains can be obtained to be 101.3, 89.8, 82.7 and 76.6 nm corresponding with the thermosets containing 5, 10, 15 and 20 wt% of PGMA-b-PDMS-b-PGMA triblock copolymer, respectively. With increasing the content of the triblock copolymer, the distance between micro phase was shortened caused by the aggregation of PDMS micro phase, which was in accordance with the analysis result of AFM. When the intermolecular interaction parameter (χ) of PDMS block in epoxy was higher than that of PGMA block in epoxy matrix, which can be calculated depending on solubility parameters, the separation of PDMS microphase could be surrounded by the miscible PGMA subchains and the separation has appeared before curing reaction because the formation of nanophase was drove by intermolecular specific interactions physically, indicating the formation mechanism of nanostructures in the epoxy containing triblock copolymer was self-assembly depicted in Scheme 2. The phase separation of the PDMS domain was restricted, which was due to the fact that the connection between PDMS block and PGMA block was a covalent bond.
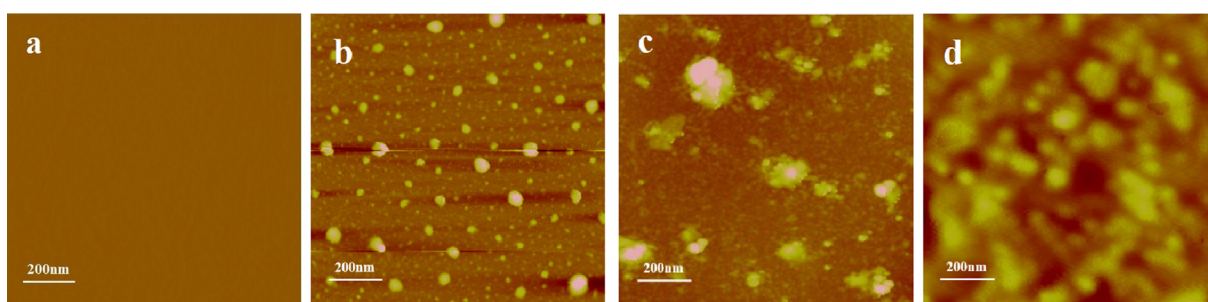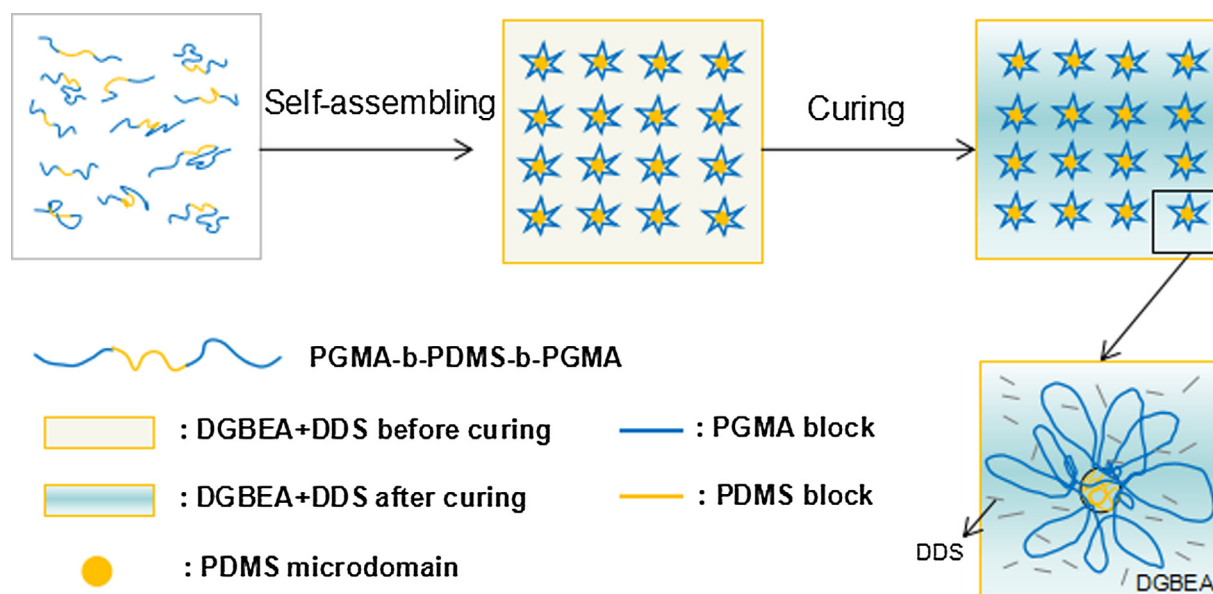

Fig. 6. AFM topography images of the epoxy thermosets with different PGMA-b-PDMS-b-PGMA contents: (a) 0, (b) 5, (c) 15, (d) 20 wt%.

Scheme 2. Schematic diagram of nanostructures during the curing reaction.

When the content of PGMA-b-PDMS-b-PGMA triblock copolymer was low, the separation could be demixed into a snowflake nanostructure, in which PDMS nanophase was surrounded by one end of dispersedly dendritic PGMA subchains (see Fig. 5b). With increasing the concentration of the triblock coploymer, the "core-shell" spherical particles in epoxy matrix: PDMS block is "spherical core" and PGMA is "spherical shell" were appeared and interconnected gradually (see Fig. 6). The snowflake nanostructure and spherical particles were fixed with the formation of a cured cross-linked structure to finally form a thermosetting resin nanocomposite in the curing reaction. And the nanostructures were clearly observed when the triblock addition amount was 5 to 25 wt% by SEM image and SAXS.

4.3. Thermal stability and mechanical properties

The glass transition temperature (Tg) of the DGEBA/PGMA-PDMS-PGMA systems were shown as in Fig. 8. It was noted that the Tg of the systems was shifted to higher temperatures with addition of the triblock copolymer between the 5–15 wt% content of the PGMA-b-PDMS-b-PGMA. The Tg of the 15 wt% and 0 wt% DGEBA/PGMA-PDMS-PGMA were 193.3 °C and 163.0 °C, respectively, indicating a excellent

improvement of epoxy matrix modified with triblock copolymer in Tg. The nanostructured epoxy thermosets possessed interesting heat resistance since the excellent heat resistance of PDMS block requiring large energy to undergo glass transition and the covalent bonding between PGMA block and epoxy network when there was few triblock copolymer. In contrast, Tg of the blends began to decrease above 20 wt% PGMA-b-PDMS-b-PGMA composition due to the plasticization of miscible PGMA segment [42].

The thermal stability of the nanodomain thermosets was investigated by means of by TGA (Fig. 9), and the thermal properties for these system were summarized in Table 1. It can be seen that the quality of the ternary blends has a mainly thermogravimetric loss between 350 and 450 °C, and the temperature of initial degradation with 5% mass loss (T_{d5}) of the epoxy thermosets containing 20 wt% triblock copolymer was 453.2 °C, far exceeding the pure epoxy resin. And the residual quality at 800 °C of the 20 wt% DGEBA/PGMA-PDMS-PGMA blends was up to 15.45% with an increase of 3.08% over the unmodified system. This can be attributed to the high heat resistance of Si-O bonds in PDMS block and the enrichment of interaction force between PGMA segment and epoxy matrix.

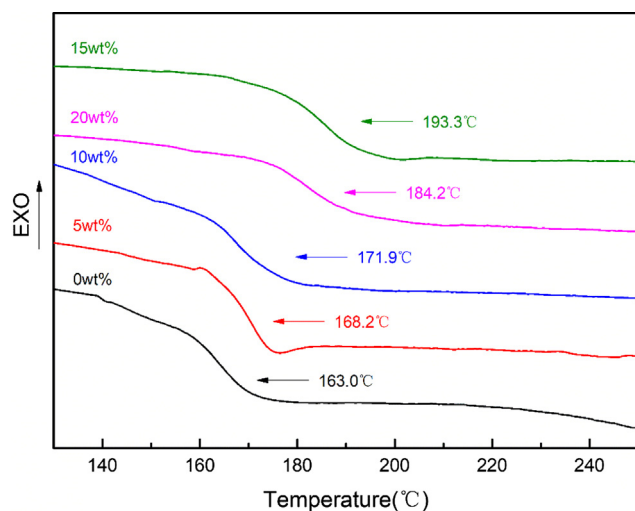The introduction of PGMA-b-PDMS-b-PGMA triblock copolymer

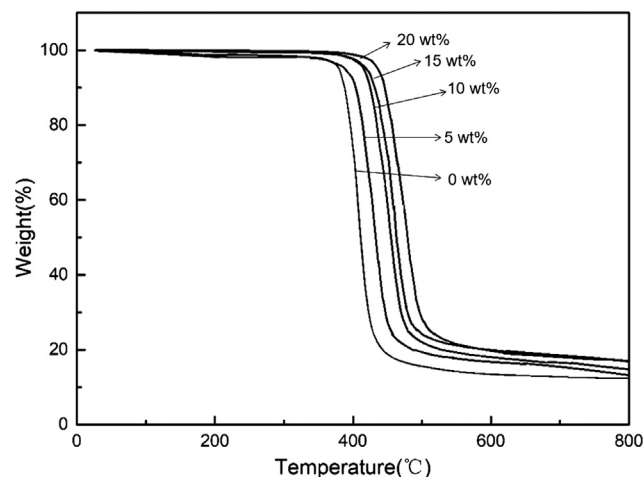**Fig. 8.** DSC spectra of DGEBA/PGMA-PDMS-PGMA.

Fig. 9. TGA curves of the DGEBA thermosets containing PGMA-b-PDMS-b-PGMA triblock copolymer.

Table 1

. TGA data of the DGEBA thermosets containing PGMA-b-PDMS-b-PGMA tri-block copolymer.

PGMA-b-PDMS-b-PGMA /wt%	T_{d5}/°C	Residue at 800 °C/%
0	385.4	12.37
5	393.0	12.49
10	414.5	13.27
15	418.8	14.95
20	435.2	15.45

Fig. 10. K_{IC} value of DGEBA/PGMA-PDMS-PGMA with different PGMA-b-PDMS-b-PGMA contents.

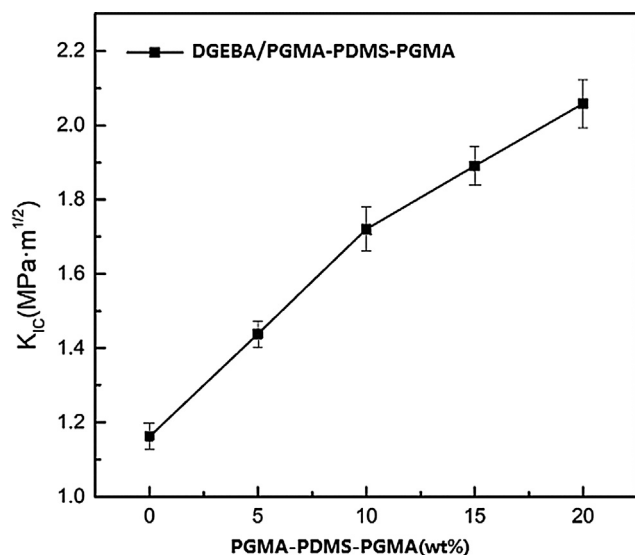**Fig. 12.** Tensile properties of DGEBA/PGMA-PDMS-PGMA with different PGMA-b-PDMS-b-PGMA contents.

into epoxy resin can increase the Tg of the blends to some extent, which also improved the fracture toughness as shown in Fig. 10. The critical stress intensity (K_{IC}), a important indicator of the toughness of the DGEBA/PGMA-PDMS-PGMA system, which shown the K_{IC} values of ternary thermosetting blends containing PGMA-b-PDMS-b-PGMA triblock copolymer was exceeding that of the neat epoxy resin, indicating the fracture toughness was eminently improved with the inclusion of the triblock copolymer. When the content of PGMA-b-PDMS-b-PGMA was 20 wt%, the K_{IC} value of the blends containing triblock copolymer peaked at 2.058 MPa·m$^{1/2}$, which was 77.1% higher than that of the neat DGEBA thermoset, since the PGMA reactive segment cross-linked with epoxy network covalent bond, which optimized the interaction between the PDMS nanophase and epoxy matrix and enhanced the interface interacti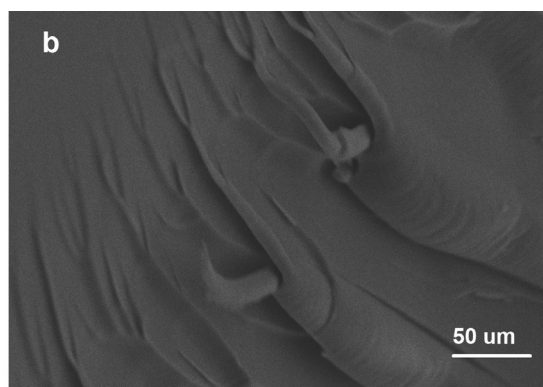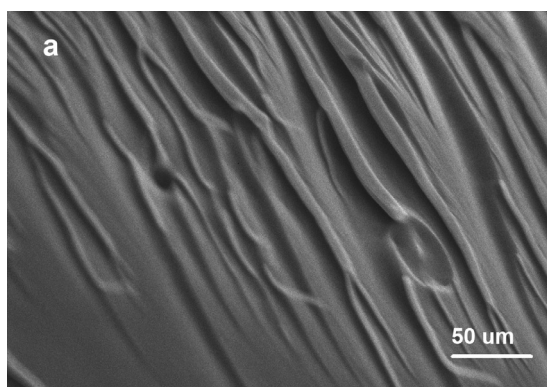ons between the epoxy matrix and plastic compatible block. According to the crack deflection mechanism, the nano-separated structure caused stress concentration, which absorbed external forces improving the toughness of the blends and the fracture toughness sectional view of pure epoxy and modified resin were demonstrated as in Fig. 11. The crack of the epoxy resin was long and sharp (Fig. 11a), indicating that the rapid development of the crack failed to induce a large amount of crazes, and the yielding phenomenon did not emerge, which was brittle fracture, while after toughening the nanodomain thermosetting crack was forficate (Fig. 11b), implying the development of craze was inhibited and disperse in all directions reducing stress concentration, which was ductile fracture.

The graph of tensile strength as a function of triblock addition was shown as in Fig. 12. It can be clearly seen that the tensile strength of thermosetting with introducing of the spherical shell nanophase was significantly improved, for example, the tensile strength of 20 wt% addition was higher 17.8% than that of pure resin, which was attributed to the chemical cross-linking point formed by epoxy group on the uniform dispersion of PGMA particle-shell and hardener interpenetrating mutually with the epoxy network, and the physical cross-linking point of the intermolecular hydrogen bonding. When the nanodomain thermosetting was subjected to applied stress, the shell portion was the stress concentration inducing local shearing yield to absorb part of the energy and the dilution of energy effectively improved the ductility and toughness of epoxy resin.

The phase behavior of the nanostructured epoxy thermosets was also investigated by DMTA. The tanδ versus temperature curves of the cured epoxy resin with different content of PGMA-b-PDMS-b-PGMA

Fig. 11. Fracture toughness sectional SEM pictures of (a) pure DGEBA and. (b) modified DGEBA with 20 wt% triblock copolymer.
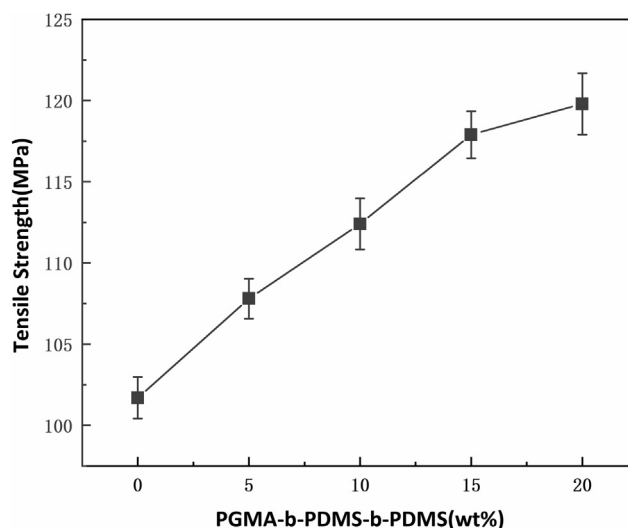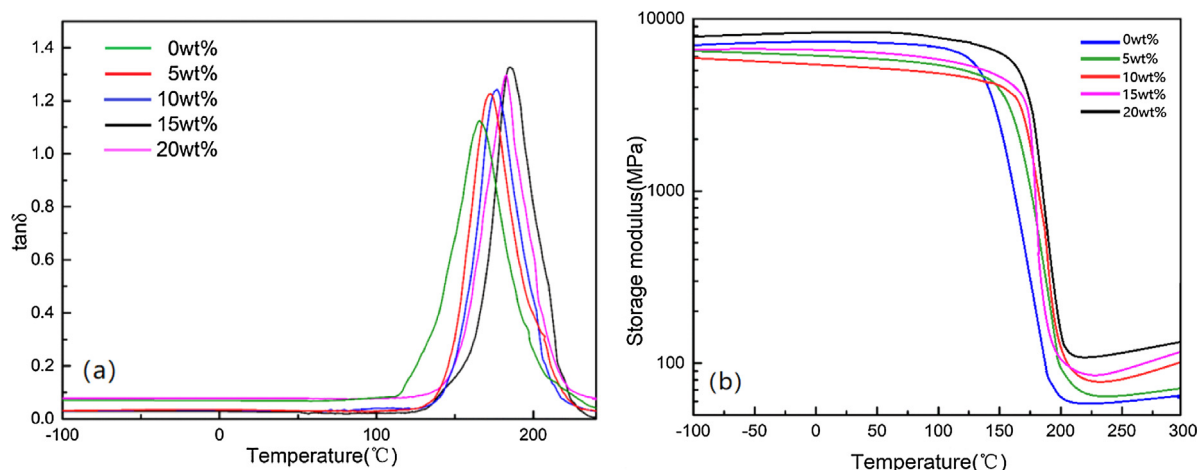
Fig. 13. DMTA curves of DGEBA/PGMA-PDMS-PGMA with different PGMA-b-PDMS-b- PGMA content: (a) loss factor tanδ, (b) storage modulus with temperature.

Table 2

. Tg and Cross-linking density of DGEBA/PGMA-PDMS-PGMA with different PGMA-b-PDMS-b-PGMA contents.

PGMA-b-PDMS-b-PGMA /wt%	Tg/°C	T/K	E(T)/MPa	$\rho/\times 10^{-3}$ mol/cm^3
0	165.7	478.9	21.5	0.92
5	172.4	485.6	50.8	2.14
10	177.2	490.4	58.2	2.43
15	196.5	509.7	90.3	3.62
20	187.7	500.9	123.4	5.04

triblock copolymer were given in Fig. 13a, where all the cured blends exhibited a well-defined relaxation peak, which corresponded to the maximum tanδ was the glass transition temperature of the system (shown in Table 2). And for neat cured epoxy, the well-defined relaxation peak centered at 165.7 °C. The addition of 15 wt% PGMA-b-PDMS-b-PGMA triblock copolymer caused a shift in Tg to a higher temperature of 196.5 °C, which were consistent with the DSC results shown in Fig. 8. It was due to the movements of the $[-Si(CH_3)_2-O-]$ and the emergence of nanoparticles, which increased the cross-link density of the system to make it harder to absorb external energy. Therefore, curing systems required higher temperatures to provide energy for glass transition. However, for blends with more than 15 wt% triblock copolymer, the Tg decreased. This can be attributed to the increase of the PGMA sub-chains in the epoxy matrix, where the flexibility of the PGMA segments played a major role with increasing the content of triblock copolymer. It can be seen from the curve of the storage modulus as a function of temperature in Fig. 13b that the stiffness of thermosetting nanoparticle blends was no significant difference with increasing the addition of the triblock copolymer, when the temperature was below 150 °C. When the test temperature was higher than the Tg of the blends, the molecular chain motion energy inside the system broken through its own energy barrier, so the storage modulus decreased significantly higher than 150 °C. Above 200 °C, the storage modulus (E) of the nanoparticle blends increased significantly with increasing the content of triblock copolymer, as the storage modulus of 20 wt% block was 123.4 MPa higher than 21.5 MPa of pure epoxy. The value of cross-linking density ρ can be calculated from the storage modulus E according to the thermodynamic analysis $\rho = E/(6RT)$, ($R = 8.314$ J mol^{-1} K^{-1}), and values were shown as in Table 2. As the content of "reactive" triblock copolymer was increased, the number of cross-linking reactive sites in equivalent mass was grow accompanied by the space of molecular chains shortened and the cross-linking density values of the modified resin increased to 4.94×10^{-3} mol/cm^3 of 20 wt% triblock from 0.90×10^{-3} mol/cm^3 of neat resin.

The mobility of molecular chains was reduce with introducing the "reactive" spherical-shell particles, which hindered development of the craze and absorbed the applied stress providing the theoretical basis for improving the fracture toughness of resin.

5. Conclusions

A triblock copolymer PGMA-b-PDMS-b-PGMA was synthesized by ATRP, which was incorporated into epoxy thermosets and the nanoparticles were obtained. Considering the difference in miscibility between PDMS and PGMA block with epoxy resin before and after curing, it was judged that the formation of the nanodomain in the thermosets was in a self-assembly manner. The DDS-cured DGEBA/PGMA-PDMS-PGMA blends showed a morphological transition from snowflake nanostructure to spherical microphase with increasing the content of PGMA-b-PDMS-b-PGMA triblock copolymer by means of SEM and AFM. Moreover, the decrease of space between neighboring nanoparticle was further verified by SAXS. It was judged that the formation of the nanodomain was successed. The TGA indicated that the heat resistance of the nanodomain in the thermosets were increased by incorporating the copolymer. The value of stress field strength factor (K_{IC}), tensile strength and storage modulus and its fracture cross-sectional view reflected the increasing trend of fracture toughness, indicating that the epoxy resin was toughened with the reactive triblock copolymer.

Acknowledgements

Appendix A. Supplementary material

Supplementary data to this article can be found online at https://doi.org/10.1016/j.eurpolymj.2019.109236.

References and notes

[1] J. Gu, X. Yang, Z. Lv, N. Li, C. Liang, Q. Zhang, Int. J. Heat Mass Transf. 92 (2016) 15–22.
[2] R. Sánchez-Hidalgo, V. Yuste-Sanchez, R. Verdejo, C. Blanco, M.A. Lopez-Manchado, R. Menéndez, Eur. Polym. J. 101 (2018) 56–65.
[3] H. He, K. Li, Polym. Compos. 33 (2012) 1755–1758.
[4] S. Qiu, W. Xing, X. Feng, B. Yu, X. Mu, R.K.K. Yuen, Y. Hu, Chem. Eng. J. 309 (2017) 802–814.
[5] A.C. Garg, Y.W. Mai, Compos. Sci. Technol. 31 (1988) 179–223.
[6] M. Stefik, S. Guldin, S. Vignolini, U. Wiesner, U. Steiner, Chem Soc Rev 44 (2015) 5076–5091.
[7] W. Fan, L. Wang, S. Zheng, Macromolecules 42 (2009) 327–336.

[8] R. Yu, S. Zheng, Macromolecules 44 (2011) 8546–8557.
[9] W. Fan, L. Wang, S. Zheng, Macromolecules 43 (2010) 10600–10611.
[10] G.M. Whitesides, B. Grzybowski, Science 295 (2002) 2418–2421.
[11] O.K. Sang, H.H. Solak, M.P. Stoykovich, N.J. Ferrier, J.J.D. Pablo, P.F. Nealey, Nature 424 (2003) 411–414.
[12] H.A. Klok, S. Lecommandoux, Adv. Mater. 13 (2010) 1217–1229.
[13] Z. Heng, Z. Zeng, B. Zhang, Y. Luo, J. Luo, Y. Chen, H. Zou, M. Liang, RSC Adv. 6 (2016) 77030–77036.
[14] C.M. Bates, C.G. Willson, Science 338 (2012) 775–779.
[15] R.S. Kumar, M. Alagar, J. Appl. Polym. Sci. 101 (2010) 668–674.
[16] K. Yamanaka, Y. Takagi, T. Inoue, Polymer 30 (1989) 1839–1844.
[17] M. Okamoto, K. Shiomi, T. Inoue, Polymer 36 (1995) 87–91.
[18] Y. Meng, X.H. Zhang, B.Y. Du, B.X. Zhou, X. Zhou, G.R. Qi, Polymer 52 (2011) 391–399.
[19] M. Blanco, M. López, R. Fernández, L. Martín, C.C. Riccardi, I. Mondragon, J. Therm. Anal. Calorim. 97 (2009) 969–978.
[20] P.A. Oyanguren, M.J. Galante, K. Andromaque, P.M. Frontini, R.J.J. Williams, Polymer 40 (1999) 5249–5255.
[21] J.L.C. And, F.C. Chang, Macromolecules (1999) 32.
[22] H.L. Huang, S.H. Goh, A.T.S. Wee, Polymer 43 (2002) 2861–2867.
[23] Q.P. Guo, H. Zheng, S. Zheng, J. Polym. Sci. Part B Polym. Phys. 41 (2003) 1085–1098.
[24] S. Zheng, N. Zhang, X. Luo, D. Ma, Polymer 36 (1995) 3609–3613.
[25] Q. Guo, C. Harrats, G. Groeninckx, H. Reynaers, M.H.J. Koch, Polymer 42 (2001) 6031–6041.
[26] Paul M. Lipic, Frank S. Bates, M.A. Hillmyer, J. Am. Chem. Soc. 120 (1998) 8963–8970.
[27] M. Blanco, M. López, G. Kortaberria, I. Mondragon, Polym. Int. 59 (2010) 523–528.
[28] H. Cong, L. Li, S. Zheng, Polymer 55 (2014) 1190–1201.
[29] Fanliang Meng, H. Sixun Zheng, Liang Li, Qi T. Liu, Macromolecules 39 (2006) 5072–5080.
[30] R. Francis, D.K. Baby, Ind. Eng. Chem. Res. 53 (2014) 17945–17951.
[31] H. Garate, I. Mondragon, N.B. D'Accorso, S. Goyanes, Macromolecules 46 (2013) 2182–2187.
[32] L. Wang, C. Zhang, H. Cong, L. Li, S. Zheng, X. Li, J. Wang, J. Phys. Chem. B 117 (2013) 8256–8268.
[33] Fanliang Meng, Sixun Zheng, Weian Zhang, Huiqin Li, Q. Liang, Macromolecules 39 (2006) 711–719.
[34] Z. Xu, S. Zheng, Macromolecules 40 (2007) 2548–2558.
[35] K. Shen, Q. Zhou, Q. Xu, D. Jiang, Z.L. Ni, Rsc Adv. 5 (2015) 61070–61080.
[36] J. Yang, Q. Zhou, K. Shen, N. Song, L. Ni, Rsc Adv. 8 (2018) 3705–3715.
[37] D.H. Builes, H. Hernandez, I. Mondragon, A. Tercjak, J. Phys. Chem. C 117 (2013) 3563–3571.
[38] Valéry Rebizant, Volker Abetz, François Tournilhac, A. François Court, L. Leibler, Macromolecules 36 (2003) 9889–9896.
[39] S. He, X. Wang, X. Guo, K. Shi, Z. Du, B. Zhang, Polym. Int. 54 (2010) 1543–1548.
[40] H. Garate, I. Mondragon, S. Goyanes, N.B. D'Accorso, J. Polym. Sci. Part A Polym. Chem. 49 (2011) 4505–4513.
[41] J.I. Meijerink, S. Eguchi, M. Ogata, T. Ishii, S. Amagi, S. Numata, H. Sashima, Polymer 35 (1994) 179–186.
[42] N. Hameed, Q. Guo, Z. Xu, T.L. Hanley, Y.W. Mai, Soft Matter 6 (2010) 6119–6129.
[43] J.X. And, K. Matyjaszewski, Eur. Polym. J. 30 (1995) 7901–7910.
[44] K. Matyjaszewski, Macromolecular Symposia 195 (2003) 25–32.
[45] Y.K. Ji, Z. Xue, S.K. Noh, W.S. Lyoo, J. Polym. Sci. Part A Polym. Chem. 49 (2008) 228–229.
[46] Q.Y. Wang, Y.F. Cao, Y. Tian, Z.L. Liu, Y. Li, F.Z. Tan, Adv. Mater. Res. 781–784 (2013) 521–525.
[47] Y. Zhao, L. Wang, A. Xiao, H. Yu, Prog. Polym. Sci. 35 (2010) 1195–1216.
[48] H. Lee, A. Joanna Pietrasik, K. Matyjaszewski, Macromolecules 39 (2006) 3914–3920.
[49] D.S. Lye, Y. Xia, M.Z. Wong, Y. Wang, M.-P. Nieh, M. Weck, Macromolecules 50 (2017) 4244–4255.